THE JOURNAL OF PHYSICAL CHEMISTRY A
A JOURNAL OF THE AMERICAN CHEMICAL SOCIETY

pubs.acs.org/JPCA

Article

Theoretical Spectroscopic Study of Two Ketones of Atmospheric Interest: Methyl Glyoxal (CH_3COCHO) and Methyl Vinyl Ketone ($CH_3COCH{=}CH_2$)

Published as part of The Journal of Physical Chemistry virtual special issue "Vincenzo Barone Festschrift".

Insaf Toumi, Samira Dalbouha, Muneerah Mogren Al-Mogren, Ounaies Yazidi, Nejm-Eddine Jaïdane, Miguel Carvajal, and María Luisa Senent*

Cite This: *J. Phys. Chem. A* 2022, 126, 7230−7241

Read Online

ACCESS | Metrics & More | Article Recommendations

ABSTRACT: Two ketones of atmospheric interest, methyl glyoxal and methyl vinyl ketone, are studied using explicitly correlated coupled cluster theory and core−valence correlation-consistent basis sets. The work focuses on the far-infrared region. At the employed level of theory, the rotational constants can be determined to within a few megahertz of the experimental data. Both molecules present two conformers, trans/cis and antiperiplanar (A_p)/synperiplanar (S_p), respectively. *trans*-Methyl glyoxal and A_p-methyl vinyl ketone are the preferred structures. *cis*-Methyl glyoxal is a secondary minimum of very low stability, which justifies the unavailability of experimental data in this form. In methyl vinyl ketone, the two conformers are almost isoenergetic, but the interconversion implies a relatively high torsional barrier of 1798 cm^{-1}. A very low methyl torsional barrier was estimated for *trans*-methyl glyoxal (V_3 = 273.6 cm^{-1}). Barriers of 429.6 and 380.7 cm^{-1} were computed for A_p- and S_p-methyl vinyl ketone. Vibrational second-order perturbation theory was applied to determine the rovibrational parameters. The far-infrared region was explored using a variational procedure of reduced dimensionality. For *trans*-methyl glyoxal, the ground vibrational state was estimated to split by 0.067 cm^{-1}, and the two low excited energy levels (1 0) and (0 1) were found to lie at 89.588 cm^{-1}/88.683 cm^{-1} (A_2/E) and 124.636 cm^{-1}/123.785 cm^{-1} (A_2/E). For A_p- and S_p-methyl vinyl ketone, the ground vibrational state splittings were estimated to be 0.008 and 0.017 cm^{-1}, respectively.

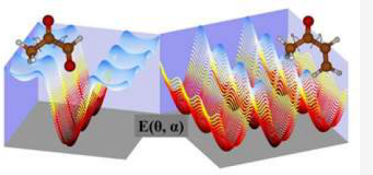

INTRODUCTION

Atmospheric processes involving volatile organic compounds (VOCs), such as the oxidation of isoprene (C_5H_8) by hydroxyl radicals and ozone, lead to the formation of methyl vinyl ketone (MVK, $CH_3COCHCH_2$, butenone), further oxidation of which produces methyl glyoxal (CH_3COCHO) and other products.[1,2] Methyl glyoxal has been recognized as an important precursor of secondary organic aerosols (SOAs) through an atmospheric heterogeneous process.[3] It has a short lifetime (∼2 h in daytime) and can also be taken up by aqueous aerosols and cloud droplets on account of their high water solubility.[3]

Thus, methyl glyoxal, which is a reduced derivative of pyruvic acid,[1] represents an atmospherically important dicarbonyl compound produced in the atmosphere from the oxidation of a number of biogenic and anthropogenic VOCs.[3] When nitrogen oxide abundances are low, acetone is an efficient secondary precursor.[3] UV photolysis and the reaction with hydroxyl radical are the main gas-phase loss processes for methyl glyoxal[1] and yield carbon monoxide, acetaldehyde, and formaldehyde.

On the other hand, MVK can originate from the primary emissions produced by fuel evaporation and combustion in urban areas and by biomass burning.[4,5] For short unsaturated ketones, atmospheric destruction is mostly controlled by the reaction with OH radicals.[6] Atmospheric oxidation of unsaturated ketones produces a variety of products following the addition of the oxidant to the double bond. Both photolysis and reaction with OH radicals are very effective loss processes for unsaturated dicarbonyls, leading to lifetimes of a few hours. The reaction of MVK with OH has been investigated in atmospheric simulation chambers.[7]

Atmospheric research on pollutants requires previous laboratory studies contemplating structural and spectroscopic properties and chemical processes. Different theoretical and experimental techniques can be employed.[6] Ab initio calculations can help the interpretation of the observations, providing viewpoints that are especially relevant for features that are difficult to address experimentally. Unfortunately, few previous works have been devoted to methyl glyoxal and MVK. The first

Received: August 8, 2022
Revised: September 9, 2022
Published: September 30, 2022

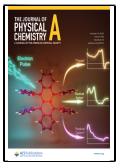

Downloaded via UNIV DE GRANADA on November 8, 2022 at 10:06:59 (UTC).
See https://pubs.acs.org/sharingguidelines for options on how to legitimately share published articles.

ACS Publications

© 2022 The Authors. Published by American Chemical Society

Table 1. CCSD(T)-F12/cc-pCVTZ-F12 Relative Energies (ΔE and ΔE^{ZPVE}, in cm^{-1}), Internal Rotation Barriers (V_3 and V^{α}, in cm^{-1}), Rotational Constants (in MHz), MP2/AVTZ Dipole Moments (in D) and Equilibrium Structural Parameters (Distances in Å and Angles in Degrees) for Methyl Glyoxal and Methyl Vinyl Ketone

	CH_3COCHO		$CH_3COCH{=}CH_2$	
parameter	trans	cis	A_p	S_p
ΔE	0.0[a]	1835	0.0[b]	196
ΔE^{ZPVE}	0.0	1747	0.0	158
θ	0.0	0.0	0.0	0.0
α	180.0	0.0	0.0	180.0
V^{α}	1980.1		1798.3	
V_3	273.6	361.9	429.6	380.7
A_e	9172.48	10470.07	9015.97	10301.29
B_e	4470.82	4061.31	4316.10	4025.09
C_e	3061.77	2979.74	2972.38	2946.60
μ_a	0.1703	2.8367	3.1006	0.6066
μ_b	0.9727	4.2102	2.2772	3.1325
μ	0.9875	5.0767	3.8469	3.1907
CH_3COCHO (C_s)				
	trans	cis		trans	cis
C2−C1	1.5254	1.5416	H5−C3−C1	109.6	109.9
C3−C1	1.4957	1.5015	H6−C3−C1	109.6	109.9
H4−C3	1.0848	1.0847	O7−C2−C1	122.7	122.3
H5−C3	1.0848	1.0913	H8−C2−C1	113.9	115.9
H6−C3	1.0848	1.0913	O9−C1−C2	117.6	119.9
O7−C2	1.2048	1.2003	H4−C3−C1−C2	180.0	180.0
H8−C2	1.1018	1.1052	H5−C3−C1−H4	121.7	121.3
O9−C1	1.2102	1.2042	H6−C3−C1−H4	−121.7	−121.3
C3−C1−C2	117.3	115.7	O7−C2−C1−C3	0.0	180.0
H4−C3−C1	109.7	110.1	H8−C2−C1−C3	180.0	0.0
$CH_3COCH{=}CH_2$ (C_s)					
	A_p	S_p		A_p	S_p
C2−C1	1.5080	1.5052	H6−C2−C1	110.5	109.7
C3−C1	1.4833	1.4924	C7−C3−C1	124.2	121.0
H4−C2	1.0851	1.0851	H8−C3−C1	114.4	117.7
H5−C2	1.0898	1.0909	H9−C7−C3	121.1	121.6
H6−C2	1.0898	1.0909	H10−C7−C3	121.7	119.7
C7−C3	1.3348	1.4924	O11−C1−C3	119.5	121.7
H8−C3	1.0823	1.0828	H4−C2−C1−C3	180.0	180.0
H9−C7	1.0803	1.0800	H5−C2−C1−H4	120.5	121.3
H10−C7	1.0810	1.0816	H6−C2−C1−H4	−120.5	−121.3
O11−C1	1.2157	1.2133	C7−C3−C1−C2	0.0	180.0
C3−C1−C2	119.1	116.1	H9−C7−C3−C1	180.0	180.0
H4−C2−C1	108.8	110.1	H10−C7−C3−C1	0.0	0.0
H5−C2−C1	110.5	109.7			

[a] E_a = −267.134470 au. [b] E_a = −231.225040 au.

electronic transitions of α,β-dicarbonyls, such as glyoxal and its methyl derivatives, have been extensively studied.[8−12] Franck−Condon analysis of methyl glyoxal shows unambiguously that excitation from the ground state to the lowest triplet state is accompanied by a rotation of the methyl group. A similar change occurs in the first excited singlet state.[8] Assignments of the electronic transitions or studies of the photodissociation processes must take into account the torsional structure of the

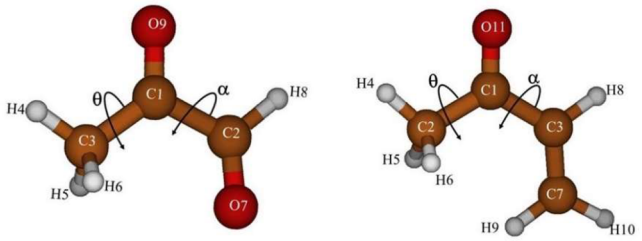

Figure 1. Atom distributions in *trans*-methyl glyoxal and Ap-MVK. The internal rotation coordinates are θ and α.

methyl derivatives.[12] Detailed assignments of the vibronic bands in the dispersed fluorescence spectra due to the $S_1(n, \pi^*) \leftarrow S_0$ transition were made. The complicated vibrational structures of the fluorescence and phosphorescence excitation spectra of methyl glyoxal and diacetyl were analyzed in terms of the internal rotational modes of the methyl group and the skeletal modes of the glyoxal framework.

The rotational and vibrational spectra of both methyl glyoxal and MVK have been previously measured and assigned.[13−23] Both molecules show two stable conformers of C_s symmetry that interconvert through large-amplitude motions, although spectroscopic data are unavailable for *cis*-methyl glyoxal. The rotational spectrum of *trans*-methyl glyoxal was first measured and assigned by Dyllick-Brenzinger and Bauder,[13] who provided the rotational constants, the components of the electric dipole moment (μ_a = 0.1597(11), μ_b = 0.9620(7)), and the internal rotation barrier (V_3 = 269.1(3) cm^{-1}). The methyl torsional fundamental was predicted at 101.6 cm^{-1} from the results of the internal rotation splittings, although a considerably higher value of 122.7 cm^{-1} was determined from the relative intensity measurements. The authors found the interaction between the methyl and skeletal torsions to be the origin of this discrepancy. Recently, Bteich et al.[14] measured the rotational spectrum in its ground vibrational state in the 4−500 GHz region. The torsion of the central bond was studied by Fateley et al.[15] Profeta et al.[16] provided the pressure-broadened quantitative infrared spectrum covering the 520−6500 cm^{-1} range with a resolution of 0.112 cm^{-1}. To complete the vibrational assignments, the far-infrared (FIR) spectrum in the 25−600 cm^{-1} region was reported in the same paper.[16]

Previous experimental[17−23] and theoretical[24−26] studies of methyl vinyl ketone are available. The IR and Raman spectra have been described.[18−20] Two stable geometries, the antiperiplanar (A_p) and synperiplanar (S_p) conformers, have been identified, although old studies attended to the most stable conformer A_p. The rotational spectrum of the A_p form was first analyzed in 1965 by Foster et al.[17] The methyl group internal rotation barrier was estimated to be V_3 = 437.19 cm^{-1} (1250 ± 20 cal/mol) and the electric dipole moment to be 3.16 ± 0.05 D.[17] The torsional splittings and the interaction between the methyl and skeletal torsions were considered in the work of Fantoni et al.[21] for the antiperiplanar form. The presence of a very stable secondary minimum was reported for the first time in 2011 in the microwave study of Wilcox et al.[22] Recently, a rotational study of both conformers was performed by Zakharenko et al.[23]

The present study is based on highly correlated ab initio calculations. The goal is to provide structural and spectroscopic theoretical data with an emphasis on the FIR region following the same procedure employed for the interconnecting carbonyl species pyruvic acid and acetone.[27−29] We study both molecules

https://doi.org/10.1021/acs.jpca.2c05653
J. Phys. Chem. A 2022, 126, 7230−7241

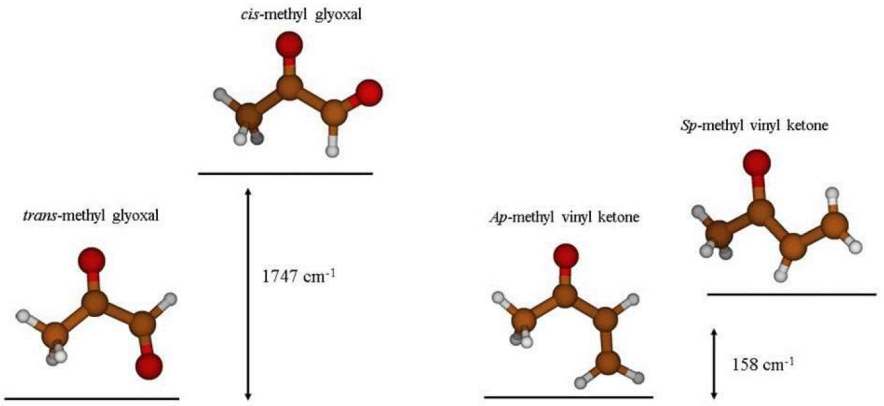

Figure 2. Relative stabilities of the conformers of methyl glyoxal and MVK.

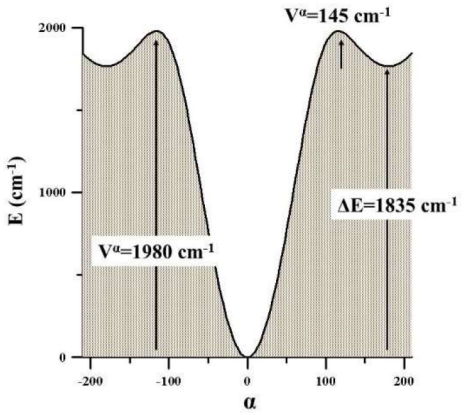

Figure 3. Energy profile for the trans → cis transformation of methyl glyoxal.

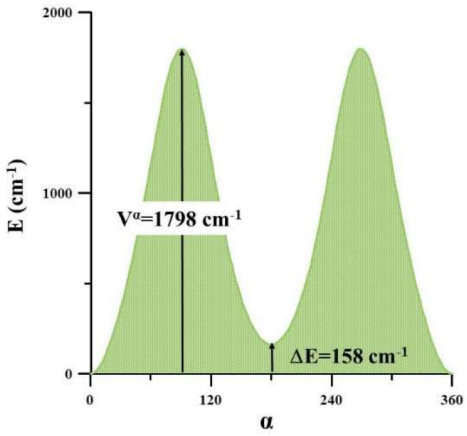

Figure 4. Energy profile for the $A_p \rightarrow S_p$ transformation of methyl vinyl ketone.

in the same paper because they share properties. Both species can be considered as acetone derivatives in which one acetone methyl group has been substituted by another functional group, −CHO or $-CH{=}CH_2$. Both species present two interacting torsional modes. The work represents a step of a general project dealing with atmospheric ketones.

We seek to underline aspects that are not fully understood or are the object of discussion. In methyl glyoxal, the cis structure is almost unidentified, and discrepancies due to the strong coupling between the two torsional modes are present in the previous assignments of the spectra of the trans structure. For both conformers, special attention is given to the FIR region. In MVK, the coupling between large-amplitude motions hinders the assignments. Both species show very low methyl torsional barriers (V_3 < 400 cm^{-1}), whose effects make interpretation difficult.

The FIR spectra of the two species are simulated using a variational procedure of reduced dimensionality implemented in an original code that uses data from ab initio calculations as input. This procedure allows us to provide information concerning the large-amplitude motions and the interactions, barriers, and torsional parameters and to map the low-lying vibrational states and their splittings. This information can be useful for the interpretation of measurements in the FIR region and also can help in the assignments of rotational and rovibrational spectra.

THEORETICAL METHODS

The geometries of the minimum-energy structures and the ab initio potential energy surfaces of reduced dimensionality were computed using explicitly correlated coupled cluster theory with single and double substitutions augmented by a perturbative treatment of triple excitations (CCSD(T)-F12b)[30,31] as implemented in Molpro[32] using default options. All of the core and valence electrons were correlated in the post-SCF process. The core−valence correlation-consistent basis set cc-pCVTZ-F12 developed for the explicitly correlated methods was employed as the basis set in connection to the additional basis sets optimized for use in the resolution of the identity.[33]

In all of the work, different levels of theory were selected by taking into consideration the required precision and the available computational tools. Second-order Møller-Plesset perturbation theory (MP2)[34] as implemented in Gaussian 16, revision C.01[35] was employed in connection with the aug-cc-pVTZ (AVTZ) basis set[36] to obtain anharmonic spectroscopic properties and the vibrational corrections for the rotational parameters and potential energy surfaces. The full-dimensional anharmonic force field was determined at all of the minima.

Vibrational second-order perturbation theory (VPT2) as implemented in Gaussian 16, revision C.01[37] was employed to obtain spectroscopic properties for the low- and medium-amplitude vibrational motions. The two torsional modes were studied variationally using the code ENEDIM[38−40] following a procedure that allows mapping of the low-lying vibrational energy levels and the splittings.

https://doi.org/10.1021/acs.jpca.2c05653
J. Phys. Chem. A 2022, 126, 7230−7241

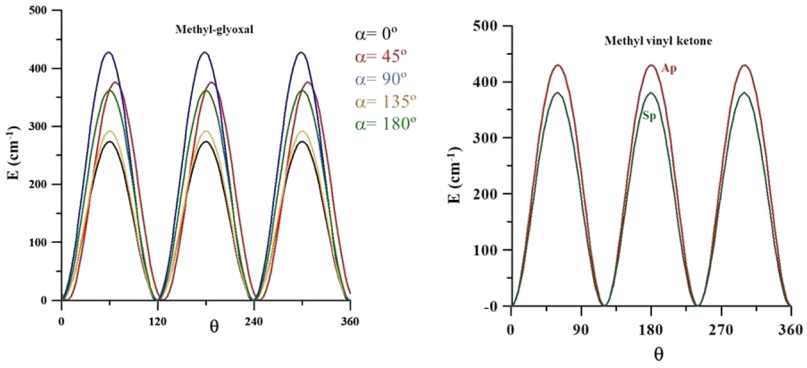

Figure 5. Methyl torsional barriers of methyl glyoxal and methyl vinyl ketone.

Table 2. Ground Vibrational State Rotational Constants (in MHz) Referred to the Principal Axis System[a]

	Methyl Glyoxal			
	trans			*cis*
constant	calcd	exptl[b]	exptl[c]	calcd
A_0	9103.21	9102.4332(31)	9108.41(15)	10391.75
B_0	4438.75	4439.8832(27)	4445.48(15)	4032.95
C_0	3039.10	3038.9404(22)	3036.778(60)	2963.05
	A_p-Methyl Vinyl Ketone			
constant	calcd	exptl[d]	exptl[e]	exptl[f]	exptl[g]
A_0	8940.41	8941.45(6)	8941.58(1)	8941.547(1)	8924.9
B_0	4275.17	4274.48(2)	4274.494(5)	4274.3593(9)	4276.8
C_0	2945.18	2945.32(2)	2945.276(4)	2945.2903(9)	2942.9
	S_p-Methyl Vinyl Ketone			
constant	calcd	exptl[f]	exptl[g]	
A_0	10236.60	10238.610(1)	10220.5	
B_0	3993.15	3991.6814(6)	3996.8	
C_0	2926.75	2925.4885(1)	2926.2	

[a]All of the experimental parameters have been transformed to be referred to the principal axis following the methods of refs 23 and 44 from the original axis systems, as indicated. [b]PAM, ref 13. [c]RAM, ref 14. [d]PAM, ref 17. [e]PAM, ref 21. [f]IAM, ref 22. [g]RAM, ref 23.

Table 3. MP2/AVTZ Quartic Centrifugal Distortion Constants[a] (in kHz) Computed Using the MP2/AVTZ Cubic Force Field

	CH_3COCHO			$CH_3COCH{=}CH_2$	
	trans		cis	A_p	S_p
constant	calcd	exptl[13]	calcd	calcd	calcd
Δ_J	1.0422	1.327(39)	0.8214	0.7953	0.7329
Δ_K	−2.2290	−1.41(70)	8.4899	0.8428	7.7405
Δ_{JK}	7.905	7.18(22)	4.8110	4.3781	2.9267
δ_J	0.3164	0.464(12)	0.2274	0.2434	0.2057
δ_K	4.5508	5.68(18)	3.0157	2.9206	2.1177

[a]Asymmetrically reduced Hamiltonian; IIIr representation.

Throughout the work, to save computational time, different levels of ab initio calculation were employed and combined. First-order parameters (structures, equilibrium rotational constants) were computed using CCSD(T)-F12 theory, whereas the vibrational corrections were determined at a lower level of theory such as MP2. Then the relevant contributions to the observable parameters were obtained and found to be very accurate. Further corrections are less dependent on the correlation energy.

RESULTS AND DISCUSSION

Structures of the Conformers. Both methyl glyoxal and MVK show two conformers, trans/cis and A_p/S_p, respectively. *trans*-Methyl glyoxal and A_p-MVK are the preferred structures. In *trans*-methyl glyoxal, "trans" refers to the relative positions of the two oxygen atoms with respect to the C1−C2 bond. In A_p-MVK, "antiperiplanar" refers to the relative positions of the two double bonds. In Table 1, the corresponding structural parameters computed at the CCSD(T)-F12/CVTZ-F12 level of theory are collected. For the computation, all of the core and valence electrons were correlated in the post-SCF process. For an easy understanding of Table 1, Figure 1 shows the atom distributions in the most stable geometries.

Table 1 shows the CCSD(T)-F12/CVTZ-F12 equilibrium rotational constants and the MP2/AVTZ components of the electric dipole moment referred to the principal axes system, the relative energies of the conformers, and the two torsional barriers, V_3 (methyl group torsion) and V^α (central bond torsion). The vibrationally corrected relative energies of the conformers are shown in Figure 2. The energy profiles accompanying the conformer conversions are represented in Figures 3 and 4.

For methyl glyoxal, the relative energy between the conformers was computed to be ΔE = 1835 cm^{-1}, and the relative

https://doi.org/10.1021/acs.jpca.2c05653
J. Phys. Chem. A 2022, 126, 7230−7241

Table 4. Anharmonic Fundamental Frequencies (in cm^{-1})[a] Calculated in This Work and Measured in Previous Experiments in the Gas Phase

		CH_3COCHO (C_s)		
		trans		*cis*
mode	assignment	calcd	exptl[16]	calcd
		A′		
1	CH_3 st	**3029**	3026.27	3028
2	CH_3 st	2939	2950.07	2228
3	CH st	2829	2828.01	**2872**
4	CO st	**1738**	1733.27	**1774**
5	CO st	1733	1729.41	**1755**
6	CH_3 b	1420	1422.92	1428
7	CH_3 b	1364	1367.38	1377
8	COH b	**1323**	1265.57	1360
9	CC st	**1228**	1228.81	**1159**
10	CH_3 b	**1002**	1005.65	**953**
11	CC st	776	781.23	**810**
12	OCC b	**567**	535.21; 591.22	634
13	CCO b	475	477.63	398
14	CCC b	268	257.76	**272**
		A″		
15	CH_3 st	2977	2977.85	2965
16	CH_3 b	**1416**	1425.22	**1433**
17	CCC b	1050	1052.04	1045
18	CO w	**881**	887.12	**869**
19	CCO b	454	480.04	**457**
20	CH_3 tor	126	121.09[16]	121
21	CC tor	96	103;[16] 105 ± 2;[15] 89[11]	41

		$CH_3COCH{=}CH_2$					
		A_p			S_p		
			exptl[19]			exptl[19]	
mode	assignment	calcd	IR	Raman	calcd	IR	Raman
		A′					
1	CH_2 st	3105	3105	3105	3111		
2	CH_2 st	**3058**	3036	3036	**3061**		
3	CH st	3021	3019	3017	3023		
4	CH_3 st	**2993**		2996	**3040**		
5	CH_3 st	2929	2936	2937	2921		
6	C═O st	**1706**	1705	1705	1730	~1729	1721
7	C═C st	1624	1620	1623	1623		
8	CH_3 b	**1449**		1426	**1427**		
9	CH_2 b	**1420**	1400	1404	1395		
10	CH_3 b	1359	1366		1352	1355	
11	CH b	**1272**		1283	1295		1298
12	CCC st	**1244**	1249	~1257	**1175**	1218	
13	CH_2 w	1052	1062	1062	1064	1180	
14	CH_3 b	935	1026		950		
15	CCC st	753	758	758	771	772	772
16	H_2CCC def	**533**	530		598	609	
17	ske def	**478**	492		410		
18	ske def	**311**	(old 413);[19] 292[b]		**273**	(old 422);[19] 272[b]	
		A″					
19	CH_3 st	2978	2971	~2955	2967		
20	CH_3 b	1434			**1444**		
21	CH_3 b	**1016**	1002		1014		
22	CH_3 b	995	987		998		
23	CH_2 b	954	950	948	973	968	
24	CH b	679	691		**658**	662	
25	OCC def	**416**	(old 292);[19] 413[b]	291	**439**	(old 272);[19] 422[b]	273
26	CH_3 tor	124	125		123	121	
27	CC tor	98	116[b]		69	87	

https://doi.org/10.1021/acs.jpca.2c05653
J. Phys. Chem. A 2022, 126, 7230−7241

Table 4. continued

[a]Mode abbreviations: st = stretching; b = bending; w = wagging; tor = torsion; def = deformation; ske def= skeletal deformation. Fermi displacements have been considered. The bands that are strongly affected by the interactions are emphasized in boldface type. [b]New assignments proposed in this work.

energy including zero-point vibrational energy was ΔE^{ZPVE} = 1747 cm^{-1}. The energy profiles shown in Figures 3, 4, and 5 are one-dimensional cuts of the potential energy surfaces described in the next sections. The barrier for the trans → cis process was estimated to be 1980 cm^{-1}, assuring the prominent feasibility of the trans form. The inverse cis → trans process, which is restricted by a very low barrier of ∼150 cm^{-1}, can occur at very low temperatures. This draws a secondary cis minimum of very low stability and justifies the unavailability of experimental data for the cis form.

On the other hand, in MVK the A_p → S_p process shown in Figure 4 is restricted by a barrier of 1798 cm^{-1}. The A_p and S_p conformers are almost isoenergetic, but their interconversion is hampered by the relatively high torsional barrier.

The methyl torsional barriers of *trans*- and *cis*-methyl glyoxal were computed to be 273.6 and 361.9 cm^{-1} at the CCSD(T)-F12/CVTZ-F12 level of theory. For the trans form, the barrier is in very good agreement with the experimental value of 271.718(24) cm^{-1}.[14] In A_p- and S_p-MVK, these parameters were estimated to be 429.6 and 380.7 cm^{-1}, respectively, which can be compared with the experimental values of 443.236(78) and 385.28(30) cm^{-1}, respectively.[23] Contrary to what is usual, there is better agreement between the calculated and experimental values for the secondary minimum than for the preferred one. It must be considered that the two structures are almost isoenergetic.[41] Figure 5 shows the energy variation with the internal rotation of the methyl groups computed for different α values. Differences between the profiles denote the potential interactions between the two torsional modes of each molecule.

In a previous work devoted to acetone,[28] the computed methyl torsional barrier of acetone (V_3 = 246 cm^{-1})[28] was compared with those of methyl formate (V_3 = 368 cm^{-1})[42] and dimethyl ether (V_3 = 951 cm^{-1}).[43] The theoretical work,[28] which was performed using highly correlated ab initio methods, highlighted the effects derived from the very low barrier of acetone, which made the computation of the low vibrational energy levels and the force field using numerical derivatives challenging. Effects that made the experimental spectrum assignments difficult were also observed (see ref 28 and references therein). Computations of the rovibrational parameters were less problematic for methyl formate[42] and dimethyl ether,[43] for which the barriers are higher than in acetone. Thus, *trans*-methyl glyoxal can be expected to behave like acetone. In MVK, the barriers are like that of methyl formate.

Rovibrational Parameters. The ground vibrational state rotational constants B_0 shown in Table 2 were computed using the following equation and the CCSD(T)-F12/CVTZ-F12 equilibrium rotational constants:

$$B_0 = B_e(\text{CCSD(T)-F12/CVTZ-F12}) + \Delta B^{vib}(\text{MP2/AVTZ}) \quad (1)$$

where ΔB^{vib} is the vibrational contribution derived from the VPT2 α_r^i vibration−rotation interaction parameters determined from the MP2/AVTZ cubic force field. In Table 2, the computed results are compared with experimental results. All of these experimental parameters are referred to the principal axis system, although different authors employed different definitions of the reference axis and effective Hamiltonians (principal axis method (PAM), rho axis method (RAM), or internal axis method (IAM)).

Table 5. CCSD(T)-F12/CVTZ-F12 Torsional Band Center Positions (ν, in cm^{-1}) Computed Variationally for Three Different Isotopologues and MP2/AVTZ Harmonic Frequencies (ω, in cm^{-1})

	CH_3COCHO		CD_3COCHO		$CH_3COCD^{18}O$	
mode	ω	ν (variational)	ω	ν (variational)	ω	ν (variational)
ν_{20}	131	124.6	123	117.6	126	116.8
ν_{21}	99	89.6	77	69	95	85.0

It is worth noting the very good agreement between the computed and experimental data for the three rotational constants. In previous studies, we determined the parameters discriminating valence and core electrons. Correlation effects due to the valence electrons were evaluated at the CCSD(T)-F12 level of theory, while CCSD(T) theory was used to describe the core correlation effects.[27−29,45,46] Generally, the approximation led to an error in one of the constants larger than for the other two parameters. In the present case, both correlation effects were treated together using CCSD(T)-F12 and a suitable basis set. In the absence of high-resolution IR data, the microwave parameters are the only experimental values to be compared with calculations. This at least qualitatively gives an estimation of the accuracy one should expect for the FIR predictions described in the next sections.

The computed parameters are closer to the available experimental ones derived with the PAM and IAM methods ($|B^{calcd} - B^{exptl}| < 2$ MHz) than those obtained using RAM. This last fitting procedure is more suitable for species showing low internal rotation barriers. The differences are similar for methyl glyoxal, showing a lower barrier than for MVK. They can be related to the number of fitting parameters, to the MP2/AVTZ force field accuracy, or to the theoretical procedure applied for the computation of the α_r^i vibration−rotation interaction parameters developed for semirigid systems. In addition to a different model Hamiltonian, the data from refs 14 and 23 include many more and much higher energy levels obtained from microwave spectra. The constants are then expected to be more accurate but are also effective due to the RAM Hamiltonian.

Table 3 collects the quartic centrifugal distortion constants. For *trans*-methyl glyoxal, the computed values are compared with those of ref 13 obtained using the Watson asymmetrically reduced Hamiltonian.[47] Some discrepancies with the experimental data are relevant for Δ_J and Δ_K, we omit the sextic constants. The quartic centrifugal distortion constants are provided to complete the theoretical information on this research.

Vibrational Fundamentals. The vibrational energies for all of the vibrational modes were computed using the following equation:

https://doi.org/10.1021/acs.jpca.2c05653
J. Phys. Chem. A 2022, 126, 7230−7241

$$E = \sum_i \omega_i^{\text{CCSD(T)-F12}}\left(v_i + \frac{1}{2}\right) + \sum_{i \geq j} x_{ij}^{\text{MP2}}\left(v_i + \frac{1}{2}\right)\left(v_j + \frac{1}{2}\right) \quad (2)$$

where the ω_i are the harmonic fundamentals, v_i and v_j are vibrational quanta, and x_{ij} are the anharmonic constants. The "harmonic contribution" was obtained using CCSD(T)-F12/AVTZ-F12, whereas the anharmonic constants were derived using VPT2 and the MP2/AVTZ force field. The anharmonic fundamentals are shown in Table 4.

The calculated values are compared with available experimental data from refs 11, 15, and 16 in the case of methyl glyoxal and from ref 19 in the case of methyl vinyl ketone. In general, there is an expectable agreement between computations and observations for the medium and high frequencies. An exception ensues for the modes ν_{18} and ν_{25} that were assigned in ref 19 to the bands observed at 413 and 292 cm^{-1} for A_p-MVK and 422 and 272 cm^{-1} for S_p-MVK, respectively. Our computed values are ν_{18} = 311 and 273 cm^{-1} and ν_{25} = 416 and 439 cm^{-1}. Thus, on the basis of the calculations, we propose the new assignment of these two bands altering the two designated values.

Fermi displacements were predicted using VPT2 as implemented in Gaussian 16[35] and the cubic force field. Those displacements were considered to obtain the values

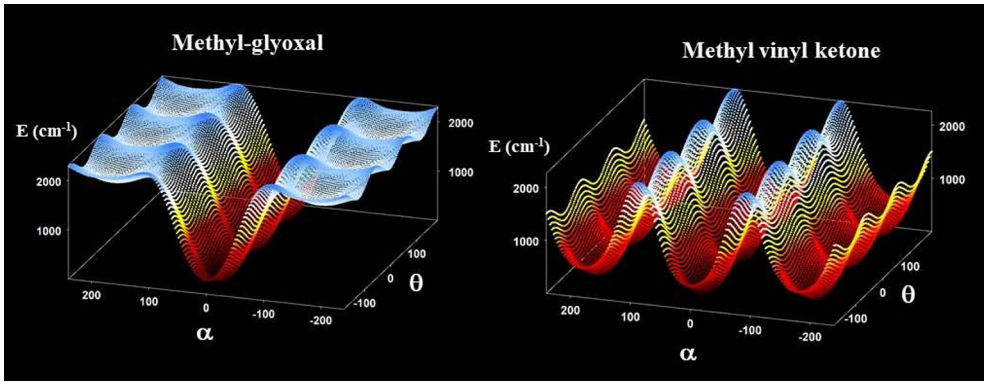

Figure 6. Two-dimensional potential energy surfaces of the methyl-glyoxal and methyl vinyl ketone.

Table 6. Low-Lying Vibrational Energy Levels of Methyl Glyoxal (in cm^{-1})

		trans-methyl glyoxal			*cis*-methyl glyoxal	
v_{21} v_{20}	symmetry	variational	VPT2	exptl	variational	VPT2
0 0	A_1	0.000			0.000	
	E	0.067			0.0025	
1 0	A_2	89.588	96	89[11]	48.111	41
	E	88.683		103[16]	48.134	
0 1	A_2	124.636	126	105 ± 2[15]	123.257	121
	E	123.785		121.09[16]		
2 0	A_1	167.682	183	167[11]	94.668	80
	E	174.832		200[11]		
1 1	A_1	198.835	213		164.690	153
	E	202.450				
0 2	A_1	242.736	229		172.366	217
	E	245.715				
3 0	A_2	261.801	260			117
	E	235.353				
v_{14}	CCC b		268	257.76[16]		262
2 1	A_2	291.883	291			184
	E	276.655				
4 0	A_1	296.141	327			152
	E	339.409				
1 2	A_2	310.899	326			252
	E	310.999				
v_{21} v_{14}			358			
0 3	A_2	356.830	364			
	E	360.716				
3 1	A_1	360.897	360			
	E	363.266				
v_{20} v_{14}			375			
2 2	A_1	397.857	396			
	E	378.421				
ZPVE		110.66			1857.52	

https://doi.org/10.1021/acs.jpca.2c05653
J. Phys. Chem. A 2022, 126, 7230−7241

Table 7. Low-Lying Vibrational Energy Levels of Methyl Vinyl Ketone (in cm^{-1})

		A_p-methyl vinyl ketone			S_p- methyl vinyl ketone		
υ_{27} υ_{26}	symmetry	variational	VPT2	exptl[19]	variational	VPT2	exptl[19]
0 0	A_1	0.000	0		0.000	0	
	E	0.008			0.017		
1 0	A_2	105.344	98	116	81.940	69	87
	E	105.354			81.954		
0 1	A_2	137.217	124	125	127.732	123	121
	E	136.869			127.130		
2 0	A_1	207.028	190		162.893	135	
	E	207.052			162.905		
1 1	A_1	237.694	217		207.448	190	
	E	237.270			207.079		
0 2	A_1	248.114	206		229.754	225	
	E	253.017			236.405		
3 0	A_2	304.548	274		243.425	203	
	E	304.599					
υ_{18}	ske def		311	292[a]		272	272[a]
2 1	A_2	344.367	303		286.179	255	
	E	349.558			285.965		
1 2	A_2	355.026	322		308.934	298	
	E	337.469			308.977		
0 3	A_2	360.806	332		342.506	331	
	E	327.644			397.294		
4 0	A_1	383.467	352		323.923	268	
	E	436.458			323.938		
υ_{27} υ_{18}			383			331	
0 4	A_1	397.545	416		421.587	416	
	E	397.415			417.881		
υ_{26} υ_{18}			412			390	
$2\upsilon_{27}$ υ_{18}						397	
υ_{25}	OCC def		416	413[a]		439	422[a]
3 1	A_1	428.394	382		364.709	319	
	E	416.985			364.354		
2 2	A_1	443.195	402		387.659	360	
	E	433.235			380.719		
1 3	A_1	455.580	414		360.184	393	
	E	448.246			317.491		
ZPVE		128.389			271.375		

[a]New assignments proposed in this work.

shown in Table 4. The bands that are strongly affected by the interactions are emphasized in boldface type.

Previous studies of *trans*-methyl glyoxal evidence disagreements for the assignments of the ν_{20} and ν_{21} torsional modes because for both normal modes the methyl and C−C CH_3 torsions present strong interactions.[13] Therefore, separability of the two torsions is not feasible. This was highlighted in ref 14, attending to the displacement **L** matrices. Then the lowest-frequency mode, assigned in ref 11 to the methyl torsional mode, is attributed in ref 14 to the C−C torsion. The present results and the analysis of the internal coordinate contributions to the normal modes, as well as the wave functions derived from the variational procedure, confirm the calculations of Bteich et al.,[14] which are in good agreement with the assignments of Profeta et al.[16] To obtain a better understanding, we determined the band positions for three different isotopic varieties using the variational procedure described below. In Table 5, the resulting frequencies are compared with harmonic frequencies computed using the MP2/AVTZ force field. Those results allow us to assign ν_{20} and ν_{21} to the methyl and C−C torsional modes, respectively.

Far-Infrared Region. The low-lying vibrational energy levels corresponding to the two torsional modes, the methyl torsion θ and the C−C torsion α, were obtained by solving the following Hamiltonian variationally:[38−40]

$$H(\theta,\alpha) = -\sum_{i=1}^{2}\sum_{j=1}^{2}\left(\frac{\partial}{\partial q_i}\right)B_{q_iq_j}(\theta,\alpha)\left(\frac{\partial}{\partial q_j}\right) + V^{\text{eff}}(\theta,\alpha) \tag{3}$$

This Hamiltonian was defined by assuming the separability of the two torsional modes from the remaining vibrational modes on the basis of vibrational energies and the predicted resonances derived from VPT2. In eq 3, $B_{q_iq_j}$ and V^{eff} are the kinetic energy parameters and the effective potential, which is defined as the sum of three contributions:

$$V^{\text{eff}}(\theta,\alpha) = V(\theta,\alpha) + V'(\theta,\alpha) + V^{\text{ZPVE}}(\theta,\alpha) \tag{4}$$

where $V(\theta,\alpha)$ is the ab initio two-dimensional potential energy surface, $V'(\theta,\alpha)$ is the Podolsky pseudopotential, and $V^{\text{ZPVE}}(\theta,\alpha)$ is the zero-point vibrational energy correction.

https://doi.org/10.1021/acs.jpca.2c05653
J. Phys. Chem. A 2022, 126, 7230−7241

The θ and α coordinates are defined as linear combinations of curvilinear internal coordinates. For methyl glyoxal, θ and α are defined as follows:

$$\theta = \frac{1}{3}(\mathrm{H4C3C1C2} + \mathrm{H5C3C1C2} + \mathrm{H6C3C1C2}) - \pi$$
$$\alpha = \mathrm{O7C2C1C3}\frac{m_O}{M} + (\mathrm{H8C2C1C3} - \pi)\frac{m_H}{M} \quad (5)$$

where m_H and m_O are the atomic masses of H and O atoms, respectively, and $M = m_O + m_H$. For methyl vinyl ketone, θ and α are defined as follows:

$$\theta = \frac{1}{3}(\mathrm{H4C2C1C3} + \mathrm{H5C2C1C3} + \mathrm{H6C2C1C3}) - \pi$$
$$\alpha = \mathrm{X_{cdm}C3C1C2} \quad (6)$$

where X_{cdm} is the center of mass of the vinyl group $CH{=}CH_2$. The two ab initio potential energy surfaces were computed using the CCSD(T)-F12/CVTZ-F12 total electronic energies of 26 geometries defined for different values of θ (0°, 90°, 180°, −90°) and α (0°, 30°, 60°, 90°, 120°, 150°, 180°). In all of these geometries, $3N_a - 8$ internal coordinates (where N_a is the number of atoms) were allowed to relax at the MP2/AVTZ level of theory. The energies were fitted to the following double Fourier series:

$$V(\theta,\alpha) = \sum_{L,M} A_{ML}^{cc} \cos L\alpha \cos 3M\theta + A_{ML}^{ss} \sin L\alpha \sin 3\theta \quad (7)$$

This function transforms as the totally symmetric representation of the G_6 molecular symmetry group.[29,48] Formally identical expressions were employed for V', V^{ZPVE}, V^{eff}, and the kinetic terms. Details concerning the computation of the Hamiltonian parameters from ab initio energies and geometries can be found in refs 39 and 40. V^{ZPVE} was computed using the MP2/AVTZ harmonic fundamentals calculated at all 26 geometries. Figure 6 presents the two effective surfaces.

Thus, for methyl glyoxal, the following expression for V^{eff} was obtained:

$$\begin{aligned} V^{eff}(\theta,\alpha) = {} & 1477.596 - 895.276\cos\alpha - 467.645\cos 2\alpha \\ & - 8.520\cos 3\alpha + 36.861\cos 4\alpha - 3.173\cos 5\alpha \\ & - 2.697\cos 6\alpha - 173.596\cos 3\theta + 0.327\cos 3\theta\cos\alpha \\ & + 27.777\cos 3\theta\cos 2\alpha + 25.259\cos 3\theta\cos 3\alpha \\ & - 12.645\cos 3\theta\cos 4\alpha - 3.528\cos 3\theta\cos 5\alpha \\ & - 0.423\cos 3\theta\cos 6\alpha - 0.857\cos 6\theta \\ & + 0.627\cos 6\theta\cos\alpha - 0.675\cos 6\theta\cos 2\alpha \\ & + 1.192\cos 6\theta\cos 3\alpha - 0.650\cos 6\theta\cos 4\alpha \\ & + 0.155\cos 6\theta\cos 5\alpha - 0.135\cos 6\theta\cos 6\alpha \\ & - 15.110\sin 3\theta\sin\alpha - 32.300\sin 3\theta\sin 2\alpha \\ & - 28.948\sin 3\theta\sin 3\alpha + 14.192\sin 3\theta\sin 4\alpha \\ & + 4.074\sin 3\theta\sin\alpha \end{aligned} \quad (8)$$

Equations formally identical to eq 8 were employed for the three kinetic parameters. For methyl glyoxal, the coefficients A_{00}^{cc} were computed to be $B_\theta = 5.5841$ cm^{-1}, $B_\alpha = 2.2379$ cm^{-1}, and $B_{\theta\alpha} = -0.1861$ cm^{-1}.

For methyl vinyl ketone, the following expression for V^{eff} was obtained:

$$\begin{aligned} V^{eff}(\theta,\alpha) = {} & 1054.034 - 40.533\cos\alpha - 848.461\cos 2\alpha \\ & - 27.787\cos 3\alpha + 138.468\cos 4\alpha + 3.036\cos 5\alpha \\ & - 21.375\cos 6\alpha - 187.497\cos 3\theta - 8.367\cos 3\theta\cos\alpha \\ & + 17.842\cos 3\theta\cos 2\alpha + 14.920\cos 3\theta\cos 3\alpha \\ & - 29.957\cos 3\theta\cos 4\alpha - 18.792\cos 3\theta\cos 5\alpha \\ & - 2.958\cos 3\theta\cos 6\alpha - 1.912\cos 6\theta \\ & - 1.499\cos 6\theta\cos\alpha - 2.915\cos 6\theta\cos 2\alpha \\ & - 0.130\cos 6\theta\cos 3\alpha - 2.034\cos 6\theta\cos 4\alpha \\ & - 1.617\cos 6\theta\cos 5\alpha - 0.878\cos 6\theta\cos 6\alpha \\ & + 9.111\sin 3\theta\sin\alpha - 23.514\sin 3\theta\sin 2\alpha \\ & - 14.331\sin 3\theta\sin 3\alpha + 37.487\sin 3\theta\sin 4\alpha \\ & + 27.208\sin 3\theta\sin 5\alpha \end{aligned} \quad (9)$$

For methyl vinyl ketone, the coefficients A_{00}^{cc} were computed to be $B_\theta = 5.5885$ cm^{-1}, $B_\alpha = 1.7971$ cm^{-1}, and $B_{\theta\alpha} = -0.1898$ cm^{-1}.

The energy levels shown in Tables 6 and 7 were determined by diagonalizing the Hamiltonian matrices, which factorize into blocks due to the symmetry conditions. The levels are classified using the symmetry representations of the G_6 molecular symmetry group, and the two quanta represent excitations of the C−C and methyl torsional modes. They are compared with available experimental data and with the results obtained using VPT2.

For *trans*-methyl glyoxal, the splitting of the ground vibrational state was estimated to be 0.067 cm^{-1}. The two lowest excited energy levels, (1 0) and (0 1), were computed to be 89.588 cm^{-1} (A_2) and 88.683 cm^{-1} (E) and 124.636 cm^{-1}(A_2) and 123.785 cm^{-1} (E). The low-lying energies of *cis*-methyl glyoxal are also provided in Table 6, but as has been already highlighted, the viability of this conformer is very low.

However, in MVK the two conformers show very similar stabilities. As they are separated by a relatively high barrier, the energies can be allocated as if they were two different molecules. In MVK, both modes υ_{27} and υ_{26} can be assigned as the torsional modes without any confusion. For A_p-MVK, the splitting of the ground vibrational state was estimated to be 0.008 cm^{-1}. The two low excited energy levels (1 0) and (0 1) were computed to be 105.344 cm^{-1} (A_2) and 105.354 cm^{-1} (E) and 137.217 cm^{-1} (A_2) and 136.869 cm^{-1} (E). For S_p-MVK, the splitting of the ground vibrational state was estimated to be 0.017 cm^{-1}, and the two lowest excited energy levels (1 0) and (0 1) were computed to be 81.940 cm^{-1} (A_2) and 81.954 cm^{-1} (E) and 127.732 cm^{-1} (A_2) and 127.130 cm^{-1} (E).

The two conformers A_p-MVK and S_p-MVK show very similar V_3 barriers, which were computed to be 429.6 and 380.7 cm^{-1}, respectively. On the basis of the barriers, similar splittings of the ground vibrational state will be expected. However, the ZPVEs are very different (128.389 cm^{-1} for A_p and 271.375 cm^{-1} for S_p), and when they are considered, it is easy to understand that the S_p splitting is double the A_p splitting.

CONCLUSIONS

In this study, the far-infrared spectra of methyl glyoxal and methyl vinyl ketone have been simulated using a variational procedure of reduced dimensionality starting from geometries

https://doi.org/10.1021/acs.jpca.2c05653
J. Phys. Chem. A 2022, 126, 7230−7241

and potential energy surfaces computed using highly correlated ab initio calculations. The procedure allows us to derive theoretical information concerning the large-amplitude motions and their interactions. Torsional barriers and parameters are provided. The low-lying vibrational states and their splittings have been mapped. We believe that this information can be useful for the interpretation of further measurements in the far-infrared region and also can help with assignments of rotational and rovibrational spectra.

The energy difference between the *trans*- and *cis*-methyl glyoxal conformers has been estimated to be 1747 cm^{-1}. The profile of the trans → cis process draws a secondary cis minimum of very low stability and justifies the unavailability of experimental data for the cis form. The A_p and S_p conformers of methyl vinyl ketone are almost isoenergetic, but their interconversion is hampered by a relatively high torsional barrier of 1798 cm^{-1}. The methyl torsional barriers of *trans*-methyl glyoxal, A_p-MVK, and S_p-MVK have been computed to be 273.6, 429, and 380.7 cm^{-1}, respectively.

Previous studies of methyl glyoxal showed disagreements for the assignments of the ν_{20} and ν_{21} normal modes because they cannot be understood in terms of two different local modes, one describing the CH_3 internal rotation and the other describing the C−C central bond torsion. The two internal rotations interact strongly and contribute to the two normal modes. The comparison of the computed far-infrared spectra of three different isotopic varieties helped to correlate ν_{20} to the methyl torsion and ν_{21} to the C−C torsion.

The low-lying torsional energy levels of methyl glyoxal and methyl vinyl ketone were computed variationally up to 450 cm^{-1}. The energies were assigned to the two conformers of methyl glyoxal and to the two conformers of MVK. The first excited levels of *cis*-methyl glyoxal have been computed, although the lifetime of this structure is very short. For *trans*-methyl glyoxal, the splitting of the ground vibrational state has been estimated to be 0.067 cm^{-1}. The two lowest excited energy levels (1 0) and (0 1) were computed to be 89.588/88.683 cm^{-1} (A_2/E) and 124.636/123.785 cm^{-1} (A_2/E). For MVK the splittings of the ground vibrational state have been estimated to be 0.008 cm^{-1} (A_p) and 0.017 cm^{-1} (S_p). The two lowest excited energy levels (1 0) and (0 1) of A_p-MVK were computed to be 105.344/105.354 cm^{-1} (A_2/E) and 137.217/136.869 cm^{-1} (A_2/E). For S_p-MVK, the corresponding energies are 81.940/81.954 cm^{-1} (A_2/E) and 127.732/127.130 cm^{-1} (A_2/E).

AUTHOR INFORMATION

Corresponding Author

María Luisa Senent − *Departamento de Química y Física Teóricas, Instituto de Estructura de la Materia, IEM-CSIC, 28006 Madrid, Spain; Unidad Asociada GIFMAN, CSIC-UHU, Universidad de Huelva, 21071 Huelva, Spain;* orcid.org/0000-0003-1878-7377; Email: ml.senent@csic.es

Authors

Insaf Toumi − *Laboratoire de Spectroscopie Atomique Moléculaire et Applications, Faculté des Sciences de Tunis, Université de Tunis El Manar, 2092 Tunis, Tunisia*

Samira Dalbouha − *Laboratoire de Spectroscopie, Modélisation Moléculaire, Matériaux, Nanomatériaux, Eau et Environnement, LS3MN2E/CERNE2D, Faculté des Sciences Rabat, Université Mohammed V de Rabat, BP 1014 Rabat, Morocco; Laboratoire de Chimie Organique et de Chimie Physique, Equipe de recherche: Modélisation Moléculaire, Matériaux et Environnement, Département de chimie, Faculté des Sciences d'Agadir, Université Ibn Zohr d'Agadir, BP 8106 Agadir, Morocco*

Muneerah Mogren Al-Mogren − *Chemistry Department, Faculty of Science, King Saud University, Riyadh 11451, Kingdom of Saudi Arabia*

Ounaies Yazidi − *Laboratoire de Spectroscopie Atomique Moléculaire et Applications, Faculté des Sciences de Tunis, Université de Tunis El Manar, 2092 Tunis, Tunisia; Institut Préparatoire aux Etudes d'Ingénieurs el Manar, Université de Tunis El Manar, 2092 Tunis, Tunisia*

Nejm-Eddine Jaïdane − *Laboratoire de Spectroscopie Atomique Moléculaire et Applications, Faculté des Sciences de Tunis, Université de Tunis El Manar, 2092 Tunis, Tunisia;* orcid.org/0000-0002-8980-1087

Miguel Carvajal − *Departamento de Ciencias Integradas, Centro de Estudios Avanzados en Física, Matemática y Computación, Unidad Asociada GIFMAN, CSIC-UHU, Universidad de Huelva, 21071 Huelva, Spain; Instituto Universitario Carlos I de Física Teórica y Computacional, Universidad de Granada, 18071 Granada, Spain*

Complete contact information is available at: https://pubs.acs.org/10.1021/acs.jpca.2c05653

Notes

The authors declare no competing financial interest.

ACKNOWLEDGMENTS

This project received funding from the European Union's Horizon 2020 Research and Innovation Programme under Marie Skłodowska-Curie Grant Agreement 872081. The authors acknowledge the National Plan for Science, Technology and Innovation (MAARIFAH), King Abdulaziz City for Science and Technology, Kingdom of Saudi Arabia (Award 0061-001-01-17-2) and the Ministerio de Ciencia, Innovación y Universidades of Spain (Grants EIN2019-103072, PID2020-112887GB-I00, PID2019-104002GB-C21, and ERDF A Way of Making Europe, by the European Union Next Generation EU/PRTR). The authors acknowledge CTI (CSIC) and CESGA and the Red Española de Computación for Grants AECT-2020-2-0008 and RES-AECT-2020-3-0011 for computing facilities.

REFERENCES

(1) Koch, S.; Moortgat, G. K. Photochemistry of Methylglyoxal in the Vapor Phase. *J. Phys. Chem. A* **1998**, *102*, 9142−9153.

(2) Aschmann, S. M.; Atkinson, R. Formation Yields of Methyl Vinyl Ketone and Methacrolein from the Gas-Phase Reaction of O_3 with Isoprene. *Environ. Sci. Technol.* **1994**, *28*, 1539−1542.

(3) Fu, T.-M.; Jacob, D. J.; Wittrock, F.; Burrows, J. P.; Vrekoussis, M.; Henze, D. K. Global Budgets of Atmospheric Glyoxal and Methylglyoxal, and Implications for Formation of Secondary Organic Aerosols. *J. Geophys. Res.* **2008**, *113*, D15303.

(4) Yokouchi, Y. Seasonal and Diurnal Variation of Isoprene and its Reaction Products in a Semi-rural Area. *Atmos. Environ.* **1994**, *28*, 2651−2658.

(5) Yokelson, R. J.; Karl, T.; Artaxo, P.; Blake, D. R.; Christian, T. J.; Griffith, D. W. T.; Guenther, A.; Hao, W. M. The Tropical Forest and Fire Emissions Experiment: Overview and Airborne Fire Emission Factor Measurements. *Atmos. Chem. Phys.* **2007**, *7*, 5175−5196.

(6) Mellouki, A.; Wallington, T. J.; Chen, J. Atmospheric Chemistry of Oxygenated Volatile Organic Compounds: Impacts on Air Quality and Climate. *Chem. Rev.* **2015**, *115*, 3984−4014.

(7) Fuchs, H.; Albrecht, S.; Acir, I.−H.; Bohn, B.; Breitenlechner, M.; Dorn, H.-P.; Gkatzelis, G. I.; Hofzumahaus, A.; Holland, F.; Kaminski, A.; et al. Investigation of the Oxidation of Methyl Vinyl Ketone (MVK) by OH Radicals in the Atmospheric Simulation Chamber SAPHIR. *Atmos. Chem. Phys.* **2018**, *18*, 8001−2016.
(8) Spangler, L. H.; Pratt, D. W. Laser-induced phosphorescence spectroscopy in supersonic jets. The Lowest Triplet States of Glyoxal, Methylglyoxal, and Biacetyl. *J. Chem. Phys.* **1986**, *84*, 4789−4796.
(9) Saenger, K. L.; Barnwell, J. D.; Herschbach, D. R. Laser Excitation Spectroscopy using Warm Supersonic Beams. The $^1A_u \rightarrow {}^1A_g$ ($\pi^* \rightarrow$ n) Transition in Biacetyl and Biacetyl-d_6. *J. Phys. Chem.* **1982**, *86*, 216−220.
(10) Chaiken, J.; Gurnick, M.; McDonald, J. D. Average Singlet−Triplet Coupling Properties of Biacetyl and Methylglyoxal using Quantum Beat Spectroscopy. *J. Chem. Phys.* **1981**, *74*, 106−116.
(11) Kamei, S.; Okuyama, K.; Abe, H.; Mikami, N.; Ito, M. Mode Selectivity in Intersystem Crossing: Giyoxal, Methylglyoxal, and Biacetyl. *J. Phys. Chem.* **1986**, *90*, 93−100.
(12) Senent, M. L.; Moule, D. C.; Smeyers, Y. G.; Toro-Labbé, A.; Peñalver, F. J. A Theoretical Spectroscopic Study of the $\tilde{A}^1A_u(S_1) \rightarrow \tilde{X}^1A_g(S_0)$ n→π^* Transition in Biacetyl, $(CH_3CO)_2$. *J. Mol. Spectrosc.* **1994**, *164*, 66−78.
(13) Dyllick-Brenzinger, C. E.; Bauder, A. Microwave spectrum, Dipole Moment and Barrier to Internal Rotation of trans-Methyl Glyoxal. *Chem. Phys.* **1978**, *30*, 147−153.
(14) Bteich, S.; Goubet, M.; Motiyenko, R. A.; Margulès, L.; Huet, T. R. Vibrational Dynamic and Spectroscopic Molecular Parameters of trans-Methyl Glyoxal, a Gaseous Precursor of Secondary Organic Aerosols. *J. Mol. Spectrosc.* **2018**, *348*, 124−129.
(15) Fateley, W. G.; Harris, R. K.; Miller, F. A.; Witkowski, R. E. Torsional Frequencies in the Far Infrared-IV. Torsions Around the C-C Single Bond in Conjugated Molecules. *Spectrochim. Acta* **1965**, *21*, 231−244.
(16) Profeta, L. T. M.; Sams, R. L.; Johnson, T. J.; Williams, S. D. Quantitative Infrared Intensity Studies of Vapor-Phase Glyoxal, Methyl Glyoxal, and 2,3-Butanedione (Diacetyl) with Vibrational Assignments. *J. Phys. Chem. A* **2011**, *115*, 9886−9900.
(17) Foster, P. D.; Rao, V. M.; Curl, R. F., Jr. Microwave Spectrum of Methyl Vinyl Ketone. *J. Chem. Phys.* **1965**, *43*, 1064−1066.
(18) Bowles, A. J.; George, W. O.; Maddams, W. F. Conformations of Some ap-Unsaturated Carbonyi Compounds. Part 1. Infrared Spectra of Acraldehyde, Crotonaldehyde, Methyl Vinyl Ketone, and Ethylideneacetone. *J. Chem. Soc. B* **1969**, *0*, 810−818.
(19) Durig, J. R.; Little, T. S. Conformational Barriers to Internal Rotation and Vibrational Assignment of Methyl Vinyl Ketone. *J. Chem. Phys.* **1981**, *75*, 3660−3668.
(20) Oelichmann, H.-J.; Bougeard, D.; Schrader, B. J. Coupled Calculation of Vibrational Frequencies and Intensities. *J. Mol. Struct.* **1981**, *77*, 179−194.
(21) Fantoni, A. C.; Caminati, W.; Meyer, R. Torsional Interactions in Methyl Vinyl Ketone. *Chem. Phys. Lett.* **1987**, *133*, 27−33.
(22) Wilcox, D. S.; Shirar, A. J.; Williams, O. L.; Dian, B. C. Additional Conformer Observed in the Microwave Spectrum of Methyl Vinyl Ketone. *Chem. Phys. Lett.* **2011**, *508*, 10−16.
(23) Zakharenko, O.; Motiyenko, R. A.; Aviles-Moreno, J. R.; Huet, T. R. Conformational Landscape and Torsion−Rotation−Vibration Effects in the Two Conformers of Methyl Vinyl Ketone, a Major Oxidation Product of Isoprene. *J. Phys. Chem. A* **2017**, *121*, 6420−6428.
(24) Garcia, J. L.; Mayoral, J. A.; Salvatella, L.; Assfeld, X.; Ruiz-Lopez, M. F. On the Conformational Preferences of Unsaturated Carbonyl Compounds. An Ab Initio Study. *J.Mol. Struct.: THEOCHEM* **1996**, *362*, 187−197.
(25) Jorgensen, W. L.; Lim, D.; Blake, J. F. Ab Initio Study of Diels-Alder Reactions of Cyclopentadiene with Ethylene, Isoprene, Cyclopentadiene, Acrylonitrile, and Methyl Vinyl Ketone. *J. Am. Chem. Soc.* **1993**, *115*, 2936−2942.
(26) Bokareva, O. S.; Bataev, V. A.; Godunov, I. A. Structures and Conformational Dynamics of Monomethylated Derivatives of Acrolein: A Quantum-Chemical Study. *J. Mol. Struct.: THEOCHEM* **2009**, *913*, 254−264.
(27) Senent, M. L.; Dalbouha, S. Large Amplitude Motions of Pyruvic Acid (CH_3-CO-COOH). *Molecules* **2021**, *26*, 4269−4282.
(28) Dalbouha, S.; Al-Mogren, M. M.; Senent, M. L. Rotational and Torsional Properties of Various Monosubstituted Isotopologues of Acetone (CH_3-CO-CH_3) from Explicitly Correlated Ab Initio Methods. *ACS Earth Space Chem.* **2021**, *5*, 890−899.
(29) El Hadki, H.; Gámez, V. G.; Dalbouha, S.; Marakchi, K.; Kabbaj, O. K.; Komiha, N.; Carvajal, M.; Senent Diez, M. L. Theoretical Spectroscopic Study of Acetyl (CH_3CO), Vinoxy (CH_2COH), and 1-Methylvinoxy (CH_3COCH_2) Radicals. Barrierless Formation Processes of Acetone in the Gas Phase. *Open Res. Eur.* **2021**, *1*, 116.
(30) Adler, T. B.; Knizia, G.; Werner, H.-J. A Simple and Efficient CCSD(T)-F12 Approximation. *J. Chem. Phys.* **2007**, *127*, 221106.
(31) Knizia, G.; Adler, T. B.; Werner, H.-J. Simplified CCSD(T)-F12 Methods: Theory and Benchmarks. *J. Chem. Phys.* **2009**, *130*, 054104.
(32) Werner, H.-J.; Knowles, P. J.; Manby, F. R.; Schütz, M.; Celani, P.; Knizia, G.; Korona, T.; Lindh, R.; Mitrushenkov, A.; Rauhut, G.; et al. *MOLPRO: A Package of Ab Initio Programs*, ver. 2012.1. http://www.molpro.net.
(33) Hill, J. G.; Mazumder, S.; Peterson, K. A. Correlation Consistent Basis Sets for Molecular Core-Valence Effects with Explicitly Correlated Wave Functions: The Atoms B−Ne and Al−Ar. *J. Chem. Phys.* **2010**, *132*, 054108.
(34) Møller, C.; Plesset, M. S. Note on an Approximation Treatment for Many-Electron Systems. *Phys. Rev.* **1934**, *46*, 618−622.
(35) Frisch, M. J.; Trucks, G. W.; Schlegel, H. B.; Scuseria, G. E.; Robb, M. A.; Cheeseman, J. R.; Scalmani, G.; Barone, V.; Petersson, G. A.; Nakatsuji, H. J.; et al. *Gaussian 16*, rev. C.01; Gaussian, Inc.: Wallingford, CT, 2016.
(36) Kendall, R. A.; Dunning, T. H., Jr; Harrison, R. J. Electron aAffinities of the First-Row Atoms Revisited. Systematic Basis Sets and Wave functions. *J. Chem. Phys.* **1992**, *96*, 6796−6806.
(37) Barone, V. Anharmonic Vibrational Properties by a Fully Automated Second-Order Perturbative Approach. *J. Chem. Phys.* **2005**, *122*, 014108.
(38) Senent, M. L. *ENEDIM: A Variational Code for Non-Rigid Molecules*, 2001. http://tct1.iem.csic.es/PROGRAMAS.htm.
(39) Senent, M. L. Determination of the Kinetic Energy Parameters of Non-rigid Molecules. *Chem. Phys. Lett.* **1998**, *296*, 299−306.
(40) Senent, M. L. Ab initio Determination of the Roto-Torsional Energy Levels of trans-1,3-Butadiene. *J. Mol. Spectrosc.* **1998**, *191*, 265−275.
(41) Toumi, I.; Yazidi, O.; Jaidane, N.-E.; Al Mogren, M. M.; Francisco, J. S.; Hochlaf, M. Stereoisomers of hydroxymethanes: Probing Structural and Spectroscopic Features upon Substitution. *J. Chem. Phys.* **2016**, *145*, 244305.
(42) Senent, M. L.; Villa, M.; Meléndez, F. J.; Domínguez-Gómez, R. Ab initio Study of the Rotational-Torsional Spectrum of Methyl Format. *Astrophys. J.* **2005**, *627*, 567−576.
(43) Senent, M. L.; Moule, D. C.; Smeyers, Y. G. An Ab initio and Spectroscopic Study of Dimethyl-ether. An Analysis of the FIR and Raman Spectra. M.L. Senent, D.C. Moule and Y.G.Smeyers. *Can.J.Phys.* **1995**, *73*, 425−431.
(44) Carvajal, M.; Willaert, F.; Demaison, J.; Kleiner, I. Reinvestigation of the Ground and First Torsional State of Methylformate. *J. Mol. Spectrosc.* **2007**, *246*, 158−166.
(45) Boussessi, R.; Senent, M. L.; Jaïdane, N. Weak Intramolecular Interaction Effects on the Low Temperature Spectra of Ethylene Glycol, an Astrophysical Apecies. *J. Chem. Phys.* **2016**, *144*, 164110.
(46) Dalbouha, S.; Senent, M. L.; Komiha, N.; Domínguez-Gómez, R. Structural and Spectroscopic Characterization of Methyl Isocyanate Methyl Cyanate, Methyl Fulminate, and Acetonitrile N-oxide using Highly Correlated Ab initio Methods. *J. Chem. Phys.* **2016**, *145*, 124309.
(47) Watson, J. K. G. Determination of Centrifugal Distortion Coefficients of Asymmetric- Top Molecules. III. Sextic Coefficients. *J. Chem. Phys.* **1968**, *48*, 4517−4524.

https://doi.org/10.1021/acs.jpca.2c05653
J. Phys. Chem. A 2022, 126, 7230−7241

(48) Yazidi, O.; Senent, M. L.; Gámez, V.; Carvajal, M.; Al-Mogren, M. M. Ab initio Spectroscopic Characterization of the Radical CH_3-O-CH_2 at Low Temperatures. *J. Chem. Phys.* **2019**, *150*, 194102.

https://doi.org/10.1021/acs.jpca.2c05653
J. Phys. Chem. A 2022, 126, 7230−7241